



Contents lists available at ScienceDirect

Composites: Part B

journal homepage: www.elsevier.com/locate/compositesb

Damage mapping of GFRP via electrical resistance measurements using nanocomposite epoxy matrix systems

Christian Viets^{a,*}, Simon Kaysser^a, Karl Schulte^{a,b}

^a Institute of Polymers and Composites, Hamburg University of Technology, Denickestrasse 15, 21073 Hamburg, Germany

^b King Abdulaziz University, Jeddah, Saudi Arabia

ARTICLE INFO

Article history:

Received 7 June 2013

Received in revised form 13 August 2013

Accepted 25 September 2013

Available online xxx

Keywords:

A. Glass fibres

A. Nano-structures

B. Electrical properties

B. Delamination

Structural health monitoring (SHM)

ABSTRACT

In the present study a technique for damage detection in nanoparticle-modified glass fibre reinforced polymer (GFRP), using in-plane and through-thickness electrical resistance measurements, is presented. Via this technique barely visible impact damages could be detected, localised and characterised (*damage mapping*). Dispersion of different filler contents of MWCNT and CB was achieved in a three roll mill. GFRP laminates with the modified matrix were manufactured with VARTM. Damage detection is realised measuring the electrical resistance distribution of the specimens before and after impact and the analysis of the damage correlated relative resistance changes. For the measurement a conductive silver ink electrode grid was directly applied to the specimen's surfaces, allowing a reliable localisation of the impact damages through damage mapping. Comparison between ultrasonic C-scans and the electrical damage mapping for a majority of the specimens showed a reliable correlation in the positions of the impact related delaminations. Different nanoparticle modifications of the GFRP-laminates resulted in a significant variation of the sensitivity of the damage mapping method. The found results show a large influence of the orientation of the electrodes as well as the used nanoparticles on the evaluated damage maps. Multiple impact tests showed the suitability of the developed damage mapping-technique for the characterisation of damage propagation regarding interlaminar delaminations and surface near matrix cracks.

© 2013 Elsevier Ltd. All rights reserved.

1. Introduction

Fibre-reinforced polymers gain more and more in importance in times of growing demands of light, efficient and energy saving structures. Fibre-reinforced polymers (FRP) offer high mechanical properties at low densities, resulting in excellent specific stiffness and strength. Due to their anisotropic structure, FRP fail in a complex manner. The maintenance and non-destructive evaluation (NDE) of FRP-structures is still a highly challenging task. This results in a high potential of an efficient and reliable method for the NDE of FRP-structures to increase their reliability and lifetime.

One example for an application of GFRP with growing importance are rotor blades for wind turbines which can be subjected to impact damage. Impacts result in internal damages, such as inter-fibre failure, delaminations and fibre rupture. These may cause the abrupt failure under compressive load of the whole GFRP structure and are difficult to evaluate *in situ* with state of the art NDE methods. In order to improve safety considerations, minimise down time, avoid sudden breakdowns and optimise maintenance, structural health monitoring (SHM) of FRP structures has gained

increasing importance. Examples for NDE methods for FRP-structures are acoustic emission, thermography, X-ray, ultrasonic and optical techniques. Some of the techniques allow detailed insights in the health of FRP-structures, but most of them have serious drawbacks and are not suitable for the *in situ* health monitoring of large or complex structures. A promising approach of SHM in FRP structures is the monitoring of the electrical material properties.

One first approach towards the strain and damage sensing in FRP through electrical measurements was the usage of electrical conductive carbon fibres in CFRP [1]. Since the epoxy matrix is an electric insulator, conduction is limited to the fibres. Changes in the DC resistance could clearly be related to straining and rupture of the carbon fibres. AC and DC electrical methods have been extensively used to study the effects of different CFRP damages, e.g. delamination or matrix cracking, under static and dynamic loading conditions, on the electrical properties [2–11]. One main advantage of these methods is that the sensor is an integral part of the structure. Although these methods can offer also quite some insight into matrix related failure mechanisms, e.g. delamination, other techniques may provide a much more detailed insight into these mechanisms. Furthermore these methods are only suitable for CFRP with electrical conductive fibres. To overcome the latter restriction,

* Corresponding author. Tel.: +49 (40) 42878 8230.

E-mail address: christian.viets@tuhh.de (C. Viets).

Muto et al. [12] developed the approach of the addition of electrical resistance based sensor fibres in non-conductive GFRP for SHM purposes. The approach was for example used and further developed with carbon nanotubes (CNT)/polymer fibres as sensors by Alexopoulos et al. [13,14]. To detect interlaminar delaminations in GFRP and CFRP, Abot et al. used CNT-yarns, coated with a thin dielectric layer to isolate them from the three-dimensionally woven carbon fibres in CFRP [15]. Although these techniques are suitable for *in situ* damage sensing, they underlie significant limitations regarding the resolution, which is dependent on the density of the sensor-fibre network.

An approach for the solution of the limitation of previous damage sensing techniques is the modification of the electrical properties of the matrix by percolated nanoparticle networks. The matrix is therefore used as a sensor material. Electrical resistance measurements allow the detection of inter- and intralaminar matrix failure as well as the indirect detection of fibre failure in FRP [16] with a very high potential resolution of the technique. Due to their electrical properties and the ability to form percolated networks, carbon black (CB) and carbon nanotubes can be used for such methods.

Böger et al. showed the influence on the sensing capabilities of different nanoparticles as well as the resulting different percolated networks formed in an epoxy matrix. A high sensitivity of the sensing technique was found with a low filler content of CB or CNTs close above the percolation threshold and therefore network structures with a low density of conductive paths and a low redundancy [17]. The redundancy of the electrical conductive network is also dependent on the structure of the CNTs. Due to waviness CNTs can form a great number of contacts between them, decreasing sensitivity [18]. Böger et al. stated that delaminations in nanoparticle modified FRP result in an abrupt and significant change in the electrical resistance of the laminate in-plane and in thickness direction due to the three-dimensional distribution of the conductive paths [17].

Wardle et al. presented a damage mapping technique for a special fuzzy-fibre reinforced polymer (FFRP), aluminiumoxide-fibres with grown-on CNTs in an epoxy matrix [19]. They used a grid of silver ink line-electrodes on both surfaces of the specimen to minimise the measuring effort. Due to the very low electrical resistivity, damage mapping of FFRP is not completely analogue to GFRP with a nanoparticle-modified matrix. The good results accomplished by Wardle et al. showed the potential of damage mapping techniques with line electrodes. They determined that the length and distance of the electrodes had a significant influence on the damage mapping results, an aspect yet to be investigated. In comparison with the recently investigated method of the electrical resistivity tomography (ERT), for example by Baltopoulos et al. [20] and Ye et al. [21], such damage mapping techniques via in thickness resistivity measurements allow the detection of damages with the same sensitivity independent of their position and distance to the specimen edge. Furthermore the ERT method's ability for detecting interlaminar delaminations is questionable. Concerning this matter, Ye et al. presented the possibility to combine the ERT method with in thickness resistance measurements to localise severe impact damages in carbon black modified GFRP specimens [21].

The goal of the present work is the development of a non-destructive testing method for barely visible impact damages in GFRP-plates modified with carbon-based nanoparticles using electrical resistance measurements. In particular the influences of different types of nanoparticles and filler contents are investigated. To allow the detection and localisation of a barely visible impact damage, a grid of conductive silver ink electrodes was directly painted on the laminate. With the electrode grid it is possible to determine the local resistance changes in thickness direc-

tion due to the impact damage. These changes can be related to the two-dimensional position and the propagation of impact related delaminations.

2. Materials and specimen preparation

The epoxy resin Epikote RIMR 135 and the amine hardener RIMH 137 from Momentive, Columbus/USA was used. This epoxy matrix was especially developed to have a low viscosity for the composite production through injection methods. To allow damage detection through measurements of the electrical resistance, three types of carbon nanoparticles were used to modify the electrical properties of the epoxy matrix: 0.3 and 0.7 wt.% multiwall carbon nanotubes (MWCNT) Baytubes C150P from Bayer Material-Science, Leverkusen/Germany, 0.3 wt.% MWCNT NC7000 from Nanocyl, Belgium, and 12 wt.% carbon black Printex 300 from Orion Engineered Carbons, Hanau/Germany. The nanoparticle-modified GFRP specimens were manufactured using vacuum assisted resin transfer moulding (VARTM).

To achieve a homogeneous dispersion of the nanoparticles in the epoxy matrix, the handmixed batches of nanoparticles and epoxy resin were processed using a three roll mill [22]. The processed highly concentrated masterbatches were mixed with additional epoxy resin and amine hardener to achieve the desired weight content of nanoparticles in the epoxy matrix directly before starting the VARTM process. To avoid porosities in the specimens matrix was mixed in a laboratory vacuum stirrer. As fibre-reinforcement, 16 layers of the unidirectional glassfibre cloth type 92145 from P-D Interglas Technologies, Erbach/Germany, were stacked to achieve a final laminate architecture of [06,90]s. The produced GFRP-plates had a fibre volume content of 45%. After 48 h of curing in the mould at room temperature, the plates were removed from the mould and post-cured for 15 h at 80 °C.

Two specimens with the dimensions of $120 \times 120 \times 3 \text{ mm}^3$ from-each plate were cut from the central area. The bottom and top surfaces of each specimen were polished with a 600 and 1000 grit sandpaper and cleaned with ethyl alcohol. In order to create a grid of electrodes on both surfaces of the specimen, parallel lines (10 on each surface, width: 1 mm, distance between: 5 mm for the central 6 electrodes, 10 mm for the outer electrodes) of conductive silver ink were applied. The electrode grids on the top (side of impact) were perpendicular to the 0°-fibre direction and on the bottom (opposite side of the impact) parallel to the 0°-fibre direction. This allowed resistance measurements between two neighbouring electrodes on one surface as well as the resistance measurements between two electrodes, each on one surface of the specimen, to measure the electrical resistance at the idealised crossing point in thickness direction. To achieve a higher resolution of the damage mapping method in the central area of the specimen, where the impacts were applied, the distance between the six central electrodes was 5 mm instead of 10 mm (Fig. 1). To achieve a repeatable, reliable and highly conductive contacting between the silver ink electrodes and the measuring instruments, one piece of copper wire was directly inserted in each electrode at one edge of the specimen surface. The non-insulated copper wires were connected to the instruments by highly conductive connection clamps, avoiding direct contact between two copper wires.

3. Experimental

3.1. Damage mapping via electrical resistance measurements

To detect and localise damages in the nanoparticle-modified GFRP-specimens, the electrical resistance in thickness direction at each crossing point of the electrodes and the in-plane electrical

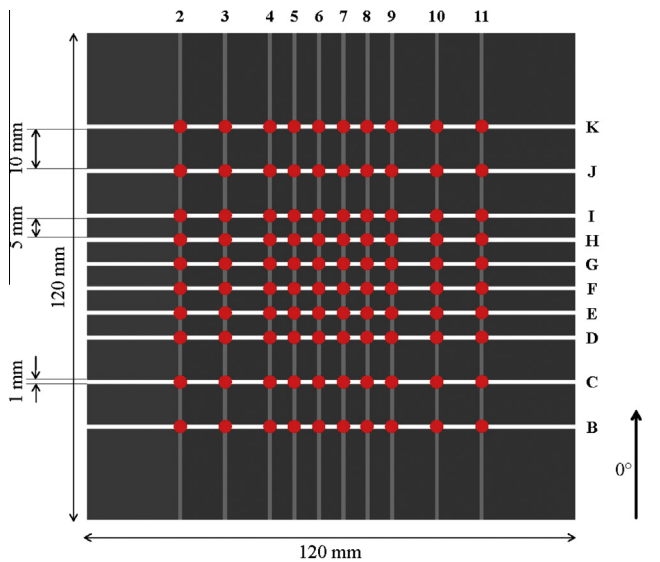


Fig. 1. Grids of conductive silver ink electrodes on the bottom (grey lines) and top side (white lines) with idealised measuring points (red points) in thickness direction at the crossings of electrodes (For interpretation of the references to colour in this figure legend, the reader is referred to the web version of this article.)

resistance between each pair of electrodes of the undamaged specimens had to be measured first. The electrical resistances were determined using a Keithley 2602 sourcemeter. A voltage of 10 V (DC) was applied to minimise the required time for the measurement of the complete grid, a switch box was used to address specific electrode pairs.

To minimise error three repeated measurements were realised and the arithmetic averages calculated. Furthermore, prior to each measurement series, the contact resistance was measured between the electrodes and the highly conductive connection clamps. The contact resistances compared to the resistance of the nanoparticle-modified GFRP-specimen were very low (up to several magnitudes difference) and were therefore neglected in the following analysis. After the complete evaluation of the electrical resistances of the undamaged specimens, a low-velocity impact damage was initiated in the centre of each nanoparticle-modified GFRP-plate using a drop weight tower with an impact energy of 7.65 J (impactor diameter 20 mm). Due to the laminate structure one impact with 7.65 J (above delamination initiating energy) induces two delaminations in the GFRP-plates between 0° and 90° -layers (Fig. 2). The electrical resistances of the impacted specimens in-plane and in thickness direction were evaluated analogously to the prior measurements allowing to calculate the resistance change in %. The relative changes in electrical resistance in thickness direction were further evaluated using the program *OriginPro 8.5* from Origin Lab Corporation. To illustrate the location, expansion and intensity

of the change in electrical resistance, two-dimensional maps, subsequently called damage maps, were created. The areas between and outside the measuring points were interpolated. Diagrams were generated from the collected data of the in-plane electrical resistances.

3.2. Ultrasonic C-scans of nanoparticle modified GFRP-specimens

To evaluate the results of the damage mapping method described in 3.1 the specimens were examined via ultrasonic C-scans using the pulse-echo-method to detect and classify the delaminations caused by impacts. The ultrasonic examinations were performed in demineralised water with the *USPC 3040*-System from *Dr. Hillger Ingenieurbüro* with the *Hillgus*-software. Due to the acoustic properties of glass fibres and the epoxy matrix as well as the highly inhomogeneous structure of GFRP, some adjustments of the ultrasonic test equipment and process were necessary for the examination of the nanoparticle-modified GFRP-plates with the available equipment. These adjustments included mainly process parameters via the *Hillgus*-software. Furthermore an ultrasonic transceiver with a frequency range of 2–7 MHz was used to optimise the testing frequency in reference to the acoustic properties of the materials. These modifications allowed a precise and reliable evaluation of the impact related delaminations in the specimens. Before inserting the impact damage, the plates were examined via ultrasonic C-scans to determine the quality of the material as well as potential failures like porosities. The second series of C-scans was taken after the impact insertion. To eliminate potential influences of water remaining in the material (e.g. due to surface cracks) the specimens were dried at least 24 h at room temperature before the resistance measurements for the damage mapping were conducted.

4. Results and discussion

4.1. Electrical properties

The damage mapping technique via electrical resistance measurements is heavily dependent on the electrical properties of the percolated particle networks in the different specimens. The filler contents of the different particles were chosen in dependence of previous works to achieve percolation and a wide range of conductivities. The DC resistances were measured with the previously described methods. Fig. 3 shows the electrical resistances in thickness direction (averaged and normalised to 10 mm distance between the electrodes). The specimens modified with 0.3 wt.% Nanocyl NC7000-MWCNTs have the lowest DC resistances (approx. 100 k Ω /10 mm). Due to the spherical geometry and the electrical properties of CB the Printex 300-modified specimen exhibit the highest electrical resistance (approx. 40,000 k Ω /10 mm). Fig. 4 shows the electrical surface resistances of the different specimens in fibre-direction and perpendicular to fibre-direction. To achieve a

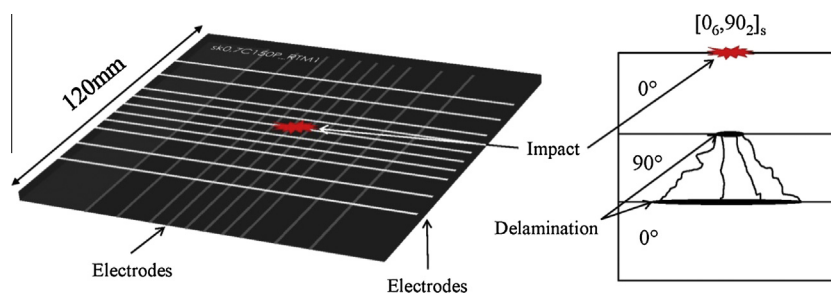


Fig. 2. Delaminations induced by central impact damage.

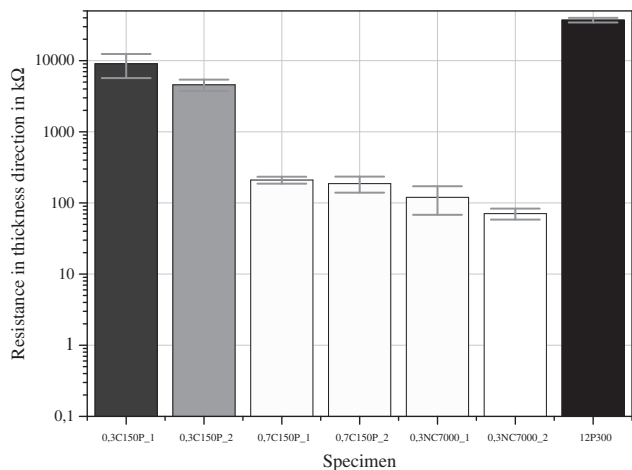


Fig. 3. Averaged electrical resistance normalised to 10 mm distance between the electrodes of the nanoparticle modified GFRP specimens in thickness direction (Filler contents: 0,3C150P: 0.3 wt.% Baytubes C150P; 0,7C150P: 0.7 wt.% Baytubes C150P; 0,3NC7000: 0.3 wt.% Nanocyl NC7000; 12P300: 12 wt.% Printex 300).

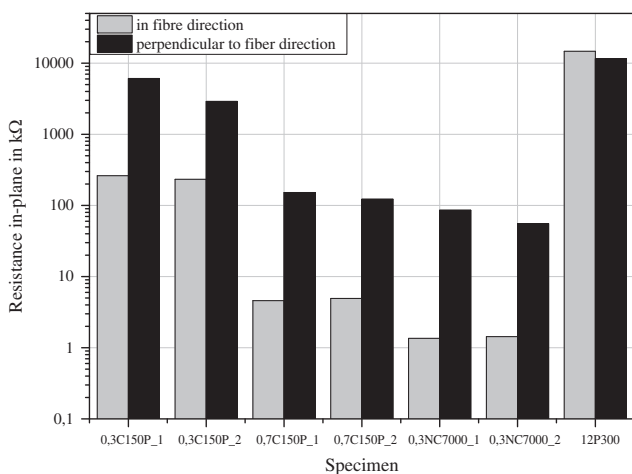


Fig. 4. Averaged in-plane electrical surface resistance normalised to 10 mm distance between the electrodes of the nanoparticle modified GFRP specimens (Filler contents: 0,3C150P: 0.3 wt.% Baytubes C150P; 0,7C150P: 0.7 wt.% Baytubes C150P; 0,3NC7000: 0.3 wt.% Nanocyl NC7000; 12P300: 12 wt.% Printex 300).

better comparability between the electrical resistances in plane (with different electrode distances) and in thickness direction, the resistances were averaged and calculated to an electrode distance of 10 mm.

It can be seen that the qualitative distribution of the resistances of the different specimens is similar to the results in thickness direction. Furthermore it can be observed that the CNT modified specimens exhibit a much larger anisotropy in the in-plane electrical resistance than the CB modified specimens. This anisotropy refers to the anisotropic formation of the CNT network due to laminate structure as well as the matrix flow direction in the VARTM process. Due to the electrode geometry a direct comparison between the in-plane and the thickness measurements is not possible. But it can be assumed that the resistivity in thickness direction is higher than in fibre direction. A detailed analysis of the electrical resistances in thickness showed an inhomogeneous resistance distribution for some specimens, presumably caused by fabrication via VARTM. To eliminate the influence of the inhomogeneous resistance distribution, the developed damage mapping technique evaluates relative changes of the local electrical resistances in unloaded conditions.

4.2. Single impact damage mapping

Goal of the presented damage mapping method was the detection and localisation of interlaminar delaminations caused by an impact. Coloured damage (resistance change) maps were created for illustration purposes. To achieve a colouration of the complete specimen surface instead of single data points, an interpolation via *OriginPro 8.5* for the regions between and outside of the data points was used. The y-direction equals the 0°-fibre direction. Fig. 5 shows the damage map of an impacted GFRP specimen with 0.7 wt.% Baytubes C150P in the epoxy matrix. It can be clearly seen, that the maximum resistance change of 9.2% occurs in the central area of the specimen where the impact was initiated (red¹ colour in Fig. 5). The resistance change in that area suggests a significant damage of the electrical conductive particle network. The black points show the idealised measuring data points. The black outline represents the outer contour of the delaminations, evaluated via ultrasonic C-scans. The damage map displays the position of the delamination and roughly the expansion of the damage in x- and y-direction. Due to the fact, that the conductive pathways of the percolated network are interrupted mostly in the area of overlapping delaminations (shown in the corresponding ultrasonic C-scans in Fig. 6), this area exhibits the highest resistance changes.

Noticeable in all generated damage maps is the exceeding elongation of the area of resistance change in y-direction compared to the damaged area in respective to the ultrasonic C-scans. This elongation can be explained by higher conductivity of the specimens in fibre direction in combination with the laminate structure and the line geometry of the electrodes which allows alternative conductive paths.

The highest resistance changes (up to 12.9%) after a single impact damage could be observed with the specimens with 0.3 wt.% Nanocyl NC7000 in the epoxy matrix. These specimens also show the most significant elongation of the damaged area due to the high anisotropy of the electrical conductivity. The specimens modified with 0.3 wt.% Baytubes C150P show a significantly lower, but still reliable, measurable resistance change of up to 3.9% and therefore a lower sensitivity to damage. On the other hand they show a more accurate illustration of the damaged area in x-direction. As expected the undamaged outer areas of most of the CNT modified specimens reveal just minor resistance changes. As illustrated in Fig. 7, the specimen with 12 wt.% Printex 300 CB in the epoxy matrix showed a slightly deviating behaviour. The area of maximum resistance change (3.6%) is not positioned at the centre of the specimen (impact point) but in the areas above and below that point. In total the CB modified specimen shows a more inhomogeneous damage map with slight resistance changes outside the delamination area. These resistance changes are possibly induced by the relatively inhomogeneous structure of the laminate due to fabrication errors such as pores, fibre undulations and filter effects caused by the high filler content used. The damage map of this material also shows the described elongation of the area of resistance change in the 0°-fibre direction. Regardless of the inhomogeneity of the material resistivities, a successful detection and localisation of the delaminations could be achieved with the developed damage mapping technique.

4.3. Detection of surface deformation and cracks

In addition to the damage mapping in thickness direction, measurements of the electrical surface resistances between electrode pairs before and after the impact damage were carried out and

¹ For interpretation of color in Fig. 5, the reader is referred to the web version of this article.

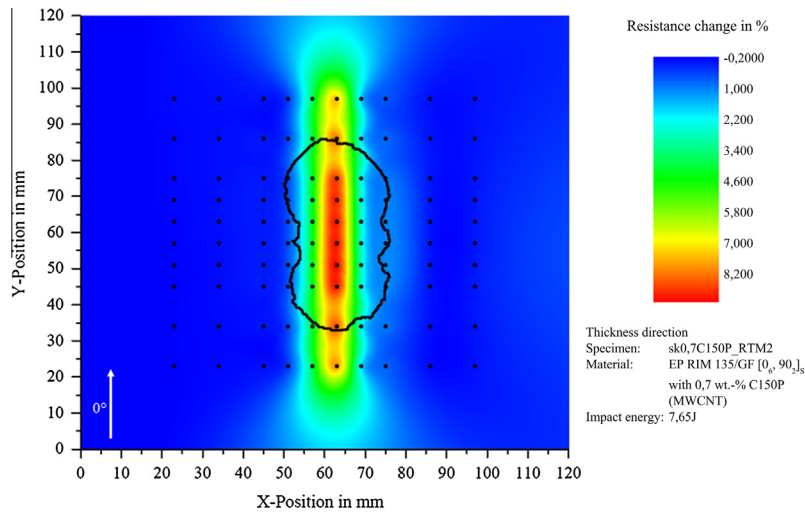


Fig. 5. Damage map of a GFRP specimen, modified with 0.7 wt.% Baytubes C150P, after impact with 7.65 J with delamination contour derived from an ultrasonic C-scan.

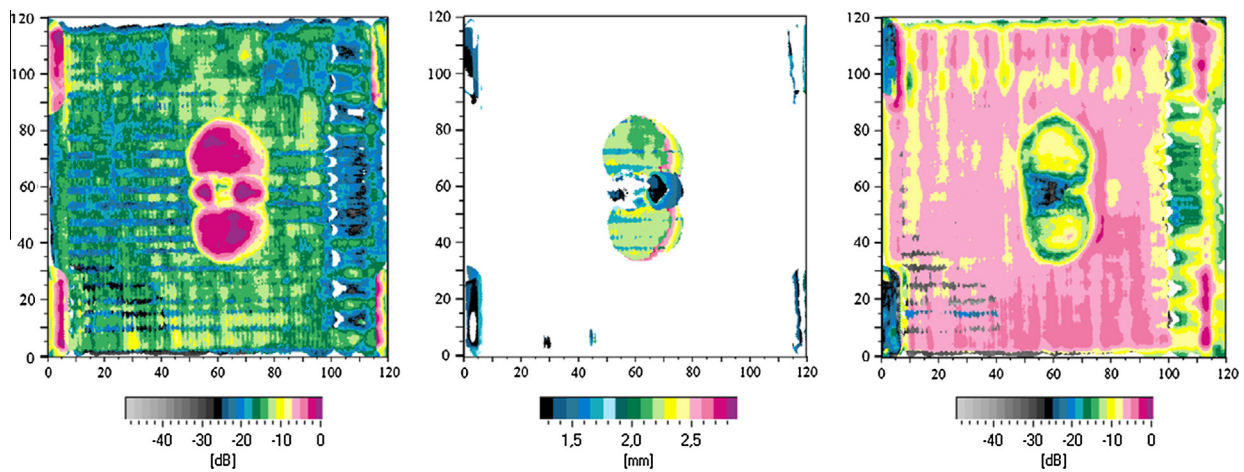


Fig. 6. Ultrasonic C-scan of GFRP specimen, modified with 0.7 wt.% Baytubes C150P, after impact with 7.65 J (left: failure echo, middle: failure depth, right: backside echo).

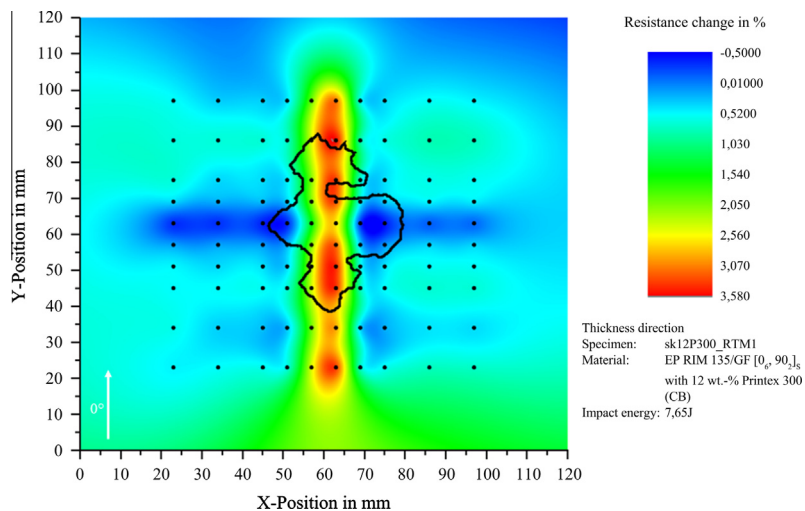


Fig. 7. Damage map of a GFRP specimen, modified with 12 wt.% Printex 300, after impact with 7.65 J with delamination contour derived from an ultrasonic C-scan.

evaluated to detect surface deformations, cracks and inter-fibre failures respectively. It should be noted that, due to the line geometry of the electrodes, only measurements of the complete surface

width and in only one direction per surface were possible. Furthermore, the damaged area is usually small compared to the length of the electrodes. The sensitivity of the resistance change for cracks

perpendicular to the electrodes, predominant on the upper surface of the specimens is therefore relatively low due to the laminate structure and the electrode placement perpendicular to the 0°-fibre direction. Fig. 8 shows the relative resistance change caused by one impact (7.65 J), measured between the electrodes on the upper surface of a specimen, modified with 0.3 wt.% C150P. It can be seen, that the most significant change in resistance (approx. –0.95%, other specimen with identical particle-modification: –1.45%), occurs in between the central pair of electrodes (F–G) due to the impact damage on the upper surface. Because cracks always lead to an increase in electrical resistance, this decrease cannot be attributed to matrix cracks. The compressive deformation of a percolated particle network can lead to a local decrease in electrical resistance as also described in [22]. Slightly visible plastic surface deformation in this area indicates such a decrease in electrical resistance due to the piezoresistive behaviour of CNT and CB nanocomposites. Bearing in mind the low geometrical fraction of the deformed area compared to the entire electrode length, the local decrease of electrical resistance has to be extensive. The other modified specimens show a similar behaviour. The highest decrease in electrical surface resistance between the central electrodes (approximately 1.55%) could be obtained with a Printex 300-modified specimen. This suggests a superior piezoresistive behaviour of CB modified over CNT modified GFRP. The with 0.3 wt.% NC7000 MWCNTs or 0.7 wt.% C150P modified specimens show electrical resistance decreases between the central electrodes on the upper surface of 0.1–0.45%.

Fig. 9 shows the relative resistance changes between the electrodes on the bottom surface of a NC7000 MWCNT modified specimen caused by one impact with 7.65 J. As it can be seen in Fig. 9 the specimen reveals a significant increase in electrical surface resistance between the central electrodes (6–7) of up to 11.4%. The increase arises from the formation of surface matrix cracks and inter-fibre failures in the lower 0°-layer parallel to the electrodes in the middle of the specimen. These are visible to the naked eye and disturb the electrical conductive pathways in the percolated particle network [22]. The other tested materials showed a similar behaviour with different sensitivities (12 wt.% Printex 300: 11.3% increase in resistance; 0.3 wt.% C150P: 0.5–3.6%; 0.7 wt.% C150P: 6.3–8.1%).

4.4. Multiple Impact damage mapping

To evaluate the influence of damage propagation on the damage mapping technique, multiple impact tests were performed.

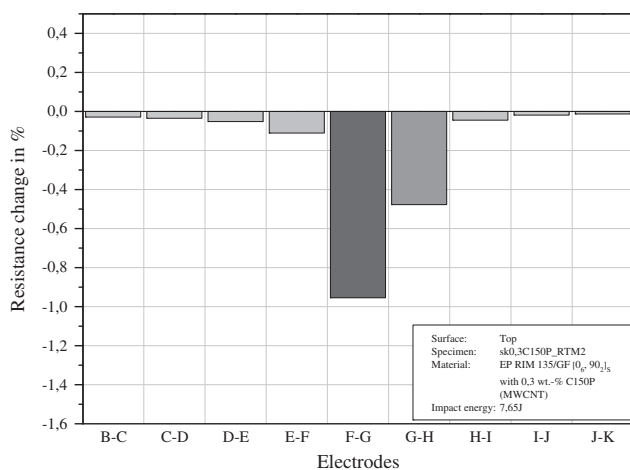


Fig. 8. Resistance change caused by impact (7.65 J) of a GFRP specimen, modified with 0.3 wt.% Baytubes C150P, measured between the electrodes on the top surface.

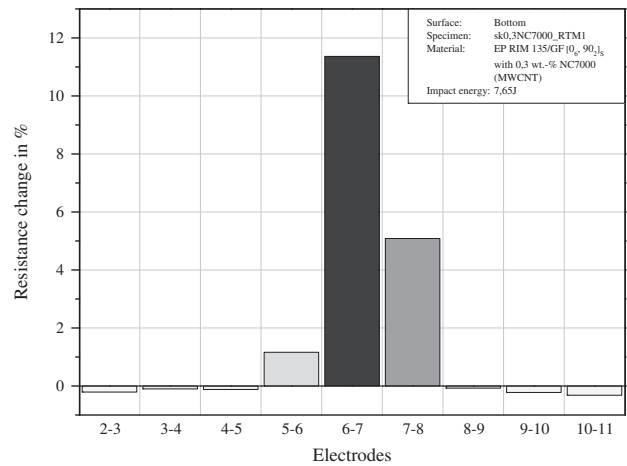


Fig. 9. Resistance change caused by impact (7.65 J) of a GFRP specimen, modified with 0.3 wt.% Nanocyl NC7000 MWCNTs, measured between the electrodes on the bottom surface.

Therefore the electrical resistances in thickness and in-plane direction of a specimen with 0.3 wt.% NC7000 in the matrix were measured before the first impact, after one impact, after 5 impacts and after 10 impacts. The low-velocity impacts had constant impact energies of 7.65 J and introduced at the approximately same position. Fig. 10 shows a comparison of the damage maps of the multiple impact tests. The relative resistance changes were calculated in reference to the resistances of the undamaged specimen. The comparison of the multiple impact damage maps in Fig. 10 shows clearly the increasing propagation of the damage and therefore the area and intensity of electrical resistance change with an increasing quantity of impacts. In the area of highest resistance change in thickness direction and therefore highest damage concentration, the maximum detected resistance change after one impact is 12.2%. After 5 impacts it increases to 19.8% and after 10 impacts to 24.6%. The area of resistance change also increased in size, which correlates with the associated ultrasonic C-scans. This leads to the conclusion that the developed damage mapping technique not only allows to detect and localise delaminations in nanoparticle-modified conductive GFRP, but also allows an analysis of the damage state and propagation relating to interlaminar delaminations. Fig. 11 shows a comparison of resistance changes between the electrodes on the bottom surface of the specimen at different impact quantities. The increasing electrical surface resistance between the central electrodes correlates with the observed increase and propagation of surface cracks in that area.

4.5. Evaluation of damage mapping technique and materials

To evaluate the suitability of the different nanocomposite matrix systems based on different carbon nanoparticles used in this work, the results of the damage mapping tests were compared. It was shown that the structure of the CNTs has a significant influence on the electric behaviour and the sensing capabilities. Specimens with a matrix modification using 0.3 wt.% Nanocyl NC7000 MWCNTs for example showed a much higher sensitivity to damage and a significantly lower electrical resistance than Baytubes C150P modified ones with an equal filler content. The main differences between NC7000 and C150P are a higher degree of agglomeration and entanglement of the Baytubes C150P as well as the higher effective aspect ratio of the NC7000 MWCNTs [23,24]. The results of these differences are a low percolation threshold for NC7000 MWCNTs [25] and, due to the fact that the resistance of nanoparticle modified epoxy is mainly determined by the number of

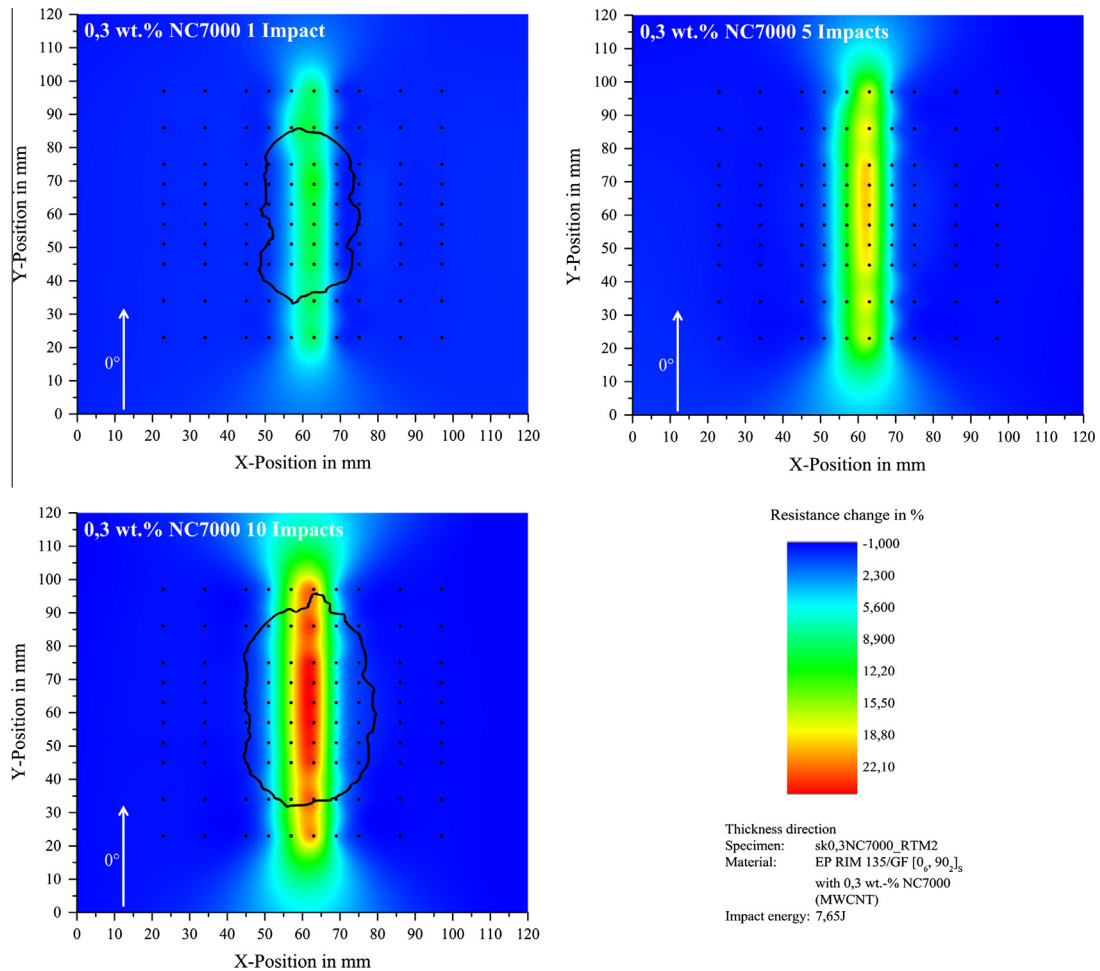


Fig. 10. Damage maps of a GFRP specimen, modified with 0.38 wt.% Nanocyl NC7000, after 1,5,10 impacts with 7.65 J with delamination contours derived from ultrasonic C-scans.

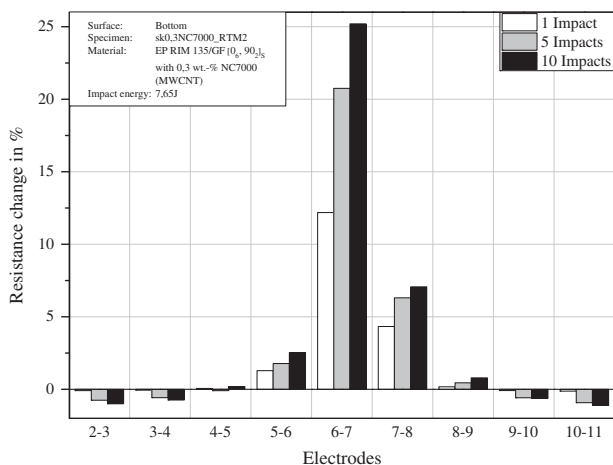


Fig. 11. Compared resistance changes between electrode pairs on the bottom surface of a specimen, modified with 0.3 wt.% NC7000, after 1, 5, 10 impacts with 7.65 J.

contact resistances between the particles [26,27], a much higher electrical conductivity. Because of the more entangled structure the percolated networks of C150P modified specimens have a higher redundancy [18] and therefore a lower sensitivity to local damage.

The difference in electrical resistance between with 0.3 wt.% and 0.7 wt.% C150P modified GFRP indicates that the percolation threshold of this nanoparticle/epoxy system lies in between these concentrations. This context offers a possible explanation for the higher sensitivity of 0.7 wt.% C150P modified GFRP over 0.3 wt.% C150P modified GFRP. Previously it was discussed, that the highest sensitivity to damage could be reached with a particle concentration near the percolation threshold [17]. The results suggest, that the filler content of 0.7 wt.% is closer to the percolation threshold.

The Printex 300-modified GFRP showed a relatively low sensitivity to damage compared to the CNT-modified specimens. Due to the fact that Printex 300 does not form a fractal particle structure [28], a high filler content was necessary to achieve sufficient electrical conductivity for the damage mapping technique. As a result of the low aspect ratio of the particles (spherical) and the high filler content, it can be assumed that the particle network of the Printex 300 modified GFRP has a high redundancy and therefore a low sensitivity to damage. Additional conductivity measurements with different filler contents showed that the percolation threshold for Printex 300 lies lower than 12 wt.%. For future works the sensitivity of this material system could be increased with lower filler contents.

Compared to the delamination contours obtained from ultrasonic C-scans, the damage maps showed an elongated form in y-direction. The source of this elongation lies first of all in the material itself as well as in the configuration of the electrodes. As the damage maps showed, the elongation of the area of significant

resistance change lies in the main fibre (0°) and injection direction. The Results showed that the electrical conductivity of the CNT-modified specimens was significantly higher in that direction, showing the higher formation of conductive pathways. If damage in percolated networks occurs, theoretically the current flows through alternative conductive pathways. Since the electrical resistance in y-direction is much lower than in x-direction, the current distributes preferably in y-direction. As consequence of the anisotropic electrical properties of the bidirectional GFRP, the electrical measurements and finally the damage mapping results reflect this anisotropy. This is shown by their smaller appearance of the damage in 90° and wider appearance in 0° -direction. The line electrodes on the bottom surface (parallel to the 0° -fibre direction) of the specimens allow a further spreading of the current flow in y-direction and therefore an undefined contact point between the percolated network in the specimen and the electrode.

In comparison to other approaches of the damage sensing in GFRP via electrical measurements, a clear and reliable detection and localisation of the damage was achieved. The resolution of this technique is solely restricted by the density of the electrode grid and the pathways in the percolated network. To achieve a similar resolution with damage sensing techniques based on electrical conductive fibres (for example [13–15]), a high density of interlaminar woven sensor fibres is necessary. This may have a negative influence on the mechanical properties. Previous studies showed that small amounts of CNTs do not degrade the mechanical properties of GFRP [17].

The assumption, that the current flows in thickness direction only at the ideal crossing points between two electrodes, cannot be verified. To avoid the resulting errors (e.g. the elongation of the area of resistance change in y-direction, in-plane detection of matrix cracks only one-dimensional), a more homogeneous conductivity of the particle network and an array of point electrodes are necessary. However, a line electrode grid has the advantage of minimal contacting effort and flexible practical application. The application of partially isolated line electrodes with only point contacts to the specimen is a promising approach for future research to combine the advantages of line and point electrodes. The electrical resistivity tomography (ERT), as presented by Baltopoulos et al. [20], offers a possible solution for the in-plane detection of damages in nanoparticle modified GFRP plates. Since the ERT shows a high potential for the in-plane detection of damages, the poor abilities of the technique to detect interlaminar damages like delaminations caused by impacts could be equalised by the additional application of the presented damage mapping technique. The lack of depth information of both techniques could be neutralised by the insertion of electrode grids between the laminate layers. In this way a three-dimensional analysis of the specimen would be possible.

5. Conclusions

This study demonstrates the high potential for the damage mapping of carbon nanoparticle modified GFRP via electrical resistance measurements for future applications in safety- or cost-relevant FRP structures as well as significant advantages over other approaches on damage sensing regarding reliability, sensitivity and practicality. The presented method can be implicated for the *in* and *ex situ* structural health monitoring of FRP-structures, only using the electrical conductive nanoparticle-modified matrix as a sensor itself without additional sensors.

The detection and localisation of barely visible impact-related damages via electrical resistance measurements was possible for all tested materials with the developed technique. Furthermore, the significant influence of the different nanoparticles and filler

contents on the results of the damage mapping, especially regarding the sensitivity of the resistance to damage, was shown. The highest impact-related change in resistance and therefore the highest sensitivity in damage detection could be reached with a Nanocyl NC7000-MWCNTs modified GF/epoxy-laminate with a filler content of 0.3 wt.%. The in-plane detection of surface near matrix cracks is also possible, but restricted by the electrode geometry. Multiple impact tests have shown that the developed damage mapping technique is suitable for the characterisation of damage propagation and accumulation regarding interlaminar delaminations and surface near matrix cracks additionally to the detection and localisation. Furthermore the detection of plastic surface deformations with electrical resistance changes was shown.

Future studies will deal with detailed investigations of the electrical properties and the sensing capabilities of nanoparticle modified GFRP and the optimisation of material systems for damage sensing application as well as the development of damage mapping techniques, which provide a three dimensional information of the damage state. To reduce the corruption of the damage mapping results due to the line geometry of the electrodes but simultaneously benefit from the minimal contacting effort, partially isolated line electrodes with point contacts to the material can be used.

References

- [1] Schulte K, Baron C. Load and failure analyses of CFRP laminates by means of electrical resistivity measurements. *Compos Sci Technol* 1989;36:63–76.
- [2] Kaddour AS, Al-Salehi FAR, Al-Hassani STS, Hinton MJ. Electrical resistance measurement technique for detecting failure in CFRP materials at high strain rate. *Compos Sci Technol* 1994;51(3):377–85.
- [3] Todoroki A, Kobayashi H, Matuura K. Application of electric potential method to smart composite structures for detecting delamination. *JSME Int J A* 1995;38(4):524–30.
- [4] Irving PE, Thiagarajan C. Fatigue damage characterization in carbon fibre composite materials using an electrical potential technique. *Smart Mater Struct* 1998;7(4):456–66.
- [5] Seo DC, Lee JJ. Damage detection of CFRP laminates using electrical resistance measurement and neural network. *Compos Struct* 1999;47:525–30.
- [6] Abry JC, Bochart S, Chateauinois A, Salvia M, Giraud G. In situ detection of damage in CFRP laminates by electrical resistance measurements. *Compos Sci Technol* 1999;59(6):925–35.
- [7] Abry JC, Choi YK, Chateauinois A, Dalloz B, Giraud G, Salvia M. In situ monitoring of damage in CFRP laminates by means of AC and DC measurements. *Compos Sci Technol* 2001;61:855–64.
- [8] Kupke M, Schulte K, Schüler R. Non-destructive testing of FRP by d.c and a.c. electrical methods. *Compos Sci Technol* 2001;61:837–47.
- [9] Todoroki A, Tanaka Y. Delamination identification of cross-ply graphite/epoxy composite beams using electrical resistance change method. *Compos Sci Technol* 2002;62:629–39.
- [10] Todoroki A, Tanaka M, Shimamura Y, Kobayashi H. Effects of delamination shape with a matrix crack on monitoring by electrical resistance method. *Adv Compos Mater* 2004;13(2):107–20.
- [11] Todoroki A, Omagari K, Shimamura Y, Kobayashi H. Matrix crack detection of CFRP using electrical resistance change with integrated surface probes. *Compos Sci Technol* 2006;66:1539–45.
- [12] Muto N, Arai Y, Shin S, Matsubara H, Yanagida H, Sugita M, et al. Hybrid composites with self-diagnosing function for preventing fatal fracture. *Compos Sci Technol* 2001;61:875–83.
- [13] Alexopoulos N, Bartholome C, Poulin P, Marioli-Riga Z. Structural health monitoring of glass fiber reinforced composites using embedded carbon nanotube (CNT) fibers. *Compos Sci Technol* 2010;70:260–71.
- [14] Alexopoulos N, Bartholome C, Poulin P, Marioli-Riga Z. Damage detection of glass fiber reinforced composites using embedded PVA-carbon nanotube (CNT) fibers. *Compos Sci Technol* 2010;70:1733–41.
- [15] Abot J, Yi S, Vatsavaya M, Medikonda S, Kier Z, Jayasinghe C, et al. Delamination detection with carbon nanotube thread in self-sensing composite materials. *Compos Sci Technol* 2010;70:1113–9.
- [16] Park J-M, Kim D-S, Kim S-J, Kim P-G, Yoon D-J, DeVries KL. Inherent sensing and interfacial evaluation of carbon nanofiber and nanotube/epoxy composites using electrical resistance measurement and micromechanical technique. *Compos Part B: Eng* 2007;38:847–61.
- [17] Böger L, Wichmann M, Meyer L, Schulte K. Load and health monitoring in glass fibre reinforced composites with an electrically conductive nanocomposite epoxy matrix. *Compos Sci Technol* 2008;68:1886–94.

- [18] Li C, Thostenson ET, Chou T-W. Sensors and actuators based on carbon nanotubes and their composites: a review. *Compos Sci Technol* 2008;68:1227–49.
- [19] Wardle B, Wicks S, Barber D, Raghavan A, Dunn C, Daniel L, Kessler S. Health monitoring of carbon nanotube (CNT) hybrid advanced composites for space applications. In: Proceedings of ECSSMMT 09 Conference, Toulouse, France; 2009.
- [20] Baltopoulos A, Polydorides N, Vavouliotis A, Kostopoulos V, Pambaguian L. Sensing capabilities of multifunctional composite materials using carbon nanotubes. In: Proceedings of International Astronautical Congress 61, Prague; 2010.
- [21] Ye L, Zhang D, Wang D, Tang Y, Mustapha S, Chen Y. Assessment of transverse impact damage in GF/EP laminates of conductive nanoparticles using electrical resistivity tomography. *Composites: Part A* 2012;43:1587–98.
- [22] Wichmann M. Electrically conductive polymer nanocomposites matrix systems with load and health monitoring capabilities. PhD thesis. Hamburg University of Technology, Institute of polymers and composites; 2009.
- [23] Bayer MaterialScience AG, Baytubes C 150 P. Agglomerate of multi-walled carbon nanotubes- preliminary data sheet for product development. Edition 2007–05-14. Bayer MaterialScience AG (Ed.), Leverkusen; 2007.
- [24] Nanocyl SA. NANOCYL NC7000 series product datasheet. Thin multi-wall carbon nanotubes. 2009–03-10-V05. Nanocyl SA, editor, Sambreville; 2009.
- [25] Bauhofer W, Kovacs J. A review and analysis of electrical percolation in carbon nanotube polymer composites. *Compos Sci Technol* 2009;69:1486–98.
- [26] Li C, Chou T. Dominant role of contact resistance in the electrical conductivity of carbon nanotube reinforced composites. *Appl Phys Lett* 2007;91:223114.
- [27] Li C, Chou T. Modeling of damage sensing in fiber composites using carbon nanotube networks. *Compos Sci Technol* 2009;68:3373–9.
- [28] Weth M, Mathias J, Emmerling A, Kuhn J, Fricke J. The structure of carbon blacks measured with (ultra)-small angle X-Ray scattering. *J Porous Mater* 2001;8:319–25.